

## The Internal Dimensions of the Cochlear Scalae With Special Reference to Cochlear Electrode Insertion Trauma

\*Slavomir Biedron, †Andreas Prescher, \*Justus Ilgner, and \*Martin Westhofen

\*Department of Otorhinolaryngology, Plastic Surgery; and †Institute of Molecular and Cellular Anatomy,  
Prosektion, RWTH Aachen University, Aachen, Germany

**Hypothesis:** To investigate the intracochlear micromorphology with regard to frequent patterns of cochlear electrode insertion trauma.

**Objective:** Cochlear implantation is a widely accepted treatment for deafness and high-grade sensorineural hearing loss. Although the device and the implantation methods are continuously optimized, damage of intracochlear structures due to electrode insertion is a frequent finding in temporal bone studies. Reduction of insertional trauma is important for the preservation of residual hearing and on the background of increasing numbers of cochlear implant recipients.

**Materials and Methods:** This study was performed with histologic specimens from the “Wittmaack temporal bone collection” (Hamburg, Germany) to examine the diameters of intracochlear spaces and to correlate the micromorphology of cochlear ducts to frequent patterns of intracochlear insertion trauma.

**Results:** The diameter of the scala tympani decreases by approximately 300  $\mu\text{m}$  during the ascending part of the basal turn. In this region, the intersegmental decrease exceeds the assumed

linear diameter decrease significantly ( $p \leq 0.001$ ). The regression of the cross-sectional diameter is accompanied by a shift of the spiral osseous lamina toward the scala tympani and by narrowing of the bony capsule of the cochlea.

**Conclusion:** Various attempts have been made to evaluate the dimensions of the cochlea related to cochlear implantation. Little attention was paid to the distinct narrowing of the scala tympani in the region of the ascending part of the cochlear duct, although from the literature, it is known that electrode insertion trauma frequently occurs here. Individual variations of the cochlear micromorphology may additionally contribute to the failure of preformed electrode arrays, but the challenge of guiding the electrode array around the first bend of the cochlear turn, that is, the pars ascendens, is obviously impaired by the interindividually constant narrowing in this area. Therefore, this finding may have implications on the development of electrode designs and insertion methods. **Key Words:** Carotid artery—Cochlea—Cochlea-carotid interval—Cochlear implant—Cross-sectional diameter—Insertional trauma—Scala tympani. *Otol Neurotol* 31:731–737, 2010.

Cochlear implantation is an established method for the treatment of patients with severe to profound hearing loss. Improved speech perception outcomes lead to a broader indication for cochlear implantation because patients with significant residual hearing become candidates for this treatment (1). Furthermore, for combined electric and acoustic stimulation, conservation of residual acoustic hearing after implantation is essential (2). On this background, it is obvious that if the number of implant recipients increases, the procedure itself must prove absolutely reliable, and preservation of functional structures of the inner ear must be accomplished.

It is known that electrode insertion trauma can cause significant degeneration of spiral ganglion cells (3). These neural structures are the target for electrical stimulation. Therefore, prevention of intracochlear insertion trauma is an important goal during cochlear implantation (4).

Efforts on improving electrode arrays and insertion techniques have been made. Adapted mechanical properties permit optimal positioning of the electrode array inside the scala tympani and help reduce insertional injury. However, even with the best available devices and skillful insertion, complete loss of residual hearing occurs in up to 10 to 20% of implantations (5). In addition, damage of inner ear structures is a frequent finding in histologic studies of temporal bones with inserted cochlear implants even if only studies with precurved electrode arrays are taken into account (6–12).

On the background of these observations, the necessity for atraumatic cochlear implantation adds further

Address correspondence and reprint requests to Slavomir Biedron, M.D., Department of Otorhinolaryngology, Plastic Surgery, RWTH Aachen University Hospital, Pauwelsstrasse 30, 52074 Aachen, Germany; E-mail: slavomir@biedron.de

relevance to systematic investigation of the inner ear anatomy. Our own studies have recently been supplemented by additional findings on anatomic variations of cochlear diameters with implication for cochlear implantation (13,14). We performed an examination of histologic temporal bone sections and measured the internal diameters of the cochlear scalae to obtain data on the relation to typical inner ear injuries caused by cochlear implantation.

## MATERIALS AND METHODS

### Material

For this study, histologic human temporal bone sections from the Wittmaack temporal bone collection (Department of History and Ethics of Medicine, University Medical Centre Hamburg-Eppendorf, Hamburg, Germany) were analyzed. The collection consists of nonpathologic and pathologic specimens. Fifty histologic series (each representing 1 sectioned human temporal bone) were chosen randomly. Of these 50 series, 22 were excluded according to the following criteria: 1) absence of glass slides containing sections of the cochlea and 2) limited assessability of cochlear morphology due to severe defects of the specimen. The remaining 28 series, which were included into the investigation, had no evidence of malformation of the labyrinth.

The number of individuals was 20. Both ears were examined in 8 cases and 1 ear only in 12 individuals. The unpaired series consisted of 8 left and 4 right temporal bones. The sex distribution in the unpaired series was 3 women, 8 men, and 1 with unknown sex, and 2 women and 6 men in the paired series. The age of the individuals ranged from 4 to 78 years (mean, 42.95 yr); for 1 individual, the age had not been documented.

### Specimen Preparation

The specimens had been prepared between 1908 and 1944 according to a histologic technique described by Eckart-Möbius (15). This procedure contained the following steps: fixation in Wittmaack fixation fluid, decalcification, celloidin embedding, serial sectioning at a thickness of 20  $\mu\text{m}$ , staining of each 4th

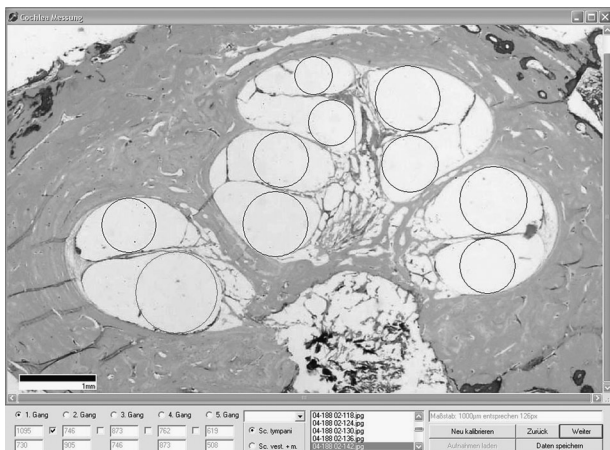


**FIG. 1.** Screenshot from the proprietary computer program interface for measurement of the cross-sectional diameters of the cochlear scalae. Superimposed circles of greatest diameter.

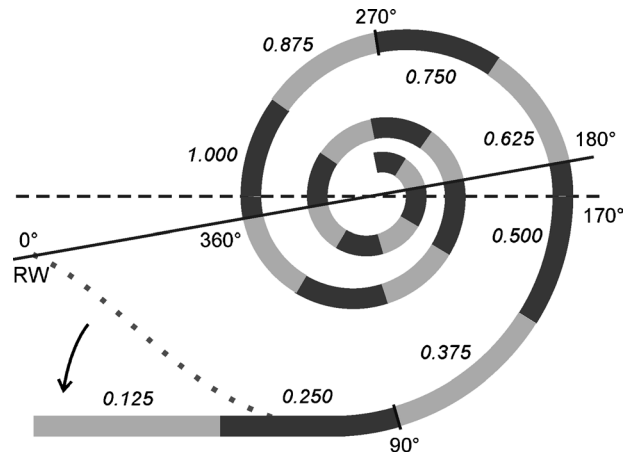


**FIG. 2.** Reconstruction of the cochlear spiral. Right human cochlea in axial view. The *dashed line* indicates the horizontal plane, whereas the *uninterrupted line* marks the reference for specifying the cochlear turns with main angles of the basal turn. The *pointed line* represents the hook region, whose course was simplified to a straight line (*arrow*). Position of the round window (RW). The segments of the cochlear spiral (see text for details) are described by 2 different shades of *gray*, with the labeling demonstrated for all segments of the basal turn.

section with hematoxylin-eosin, and mounting on covered glass slides. All cochleae were cut in the vertical plane, perpendicular to the axis of the pyramid.

### Cross-Sectional Diameters

The glass slides containing the histologic specimens were digitized by means of light microscopy (BX50, Olympus, Japan) and a color video camera (SSC-DC54P, Sony, USA), which was connected to a personal computer. For measuring the cross-sectional diameter of the cochlear scalae, a computer program was written. By means of this software, images of each histologic section were displayed, and circles were matched to the greatest diameter of the scalae using the mesothelium-like cells that line the wall of the scalae as a boundary (Fig. 1). This method was described by Walby in 1985 (16). In contrast, the author used a magnifying microprojector to project the specimens on paper to match previously prepared circles. For our study, the scala tympani and the scala vestibuli were measured.

### Graphic Reconstruction and Reference System

To analyze these measurements in reference to their original positions along the cochlear ducts, the spiral of each cochlea was reconstructed by use of semicircles, as described by Guild (17) and Schuknecht (18). Whereas the aforementioned authors described the reconstruction of the path of the organ of Corti, the path of the scalar lumen itself was reconstructed for the present work (16). Therefore, the semicircles that were used for constructing the spirals were fitted to the diameters of scala tympani half-turns. A half-turn was defined as the distance between the histologic sections where the scalar lumen was cut tangentially (16).

Figure 2 demonstrates a schematic reconstruction of the cochlear duct in axial view (according to the axis of the modiolus). The base of the spiral was set on that particular section on which the most distal part of the round window membrane was found. Positions on the spiral were specified in terms of

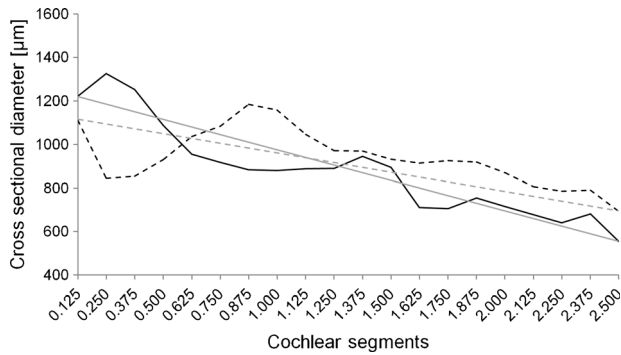


**FIG. 3.** Cross-sectional diameter of greatest circle fitted into the scala tympani (solid curve) and the scala vestibuli (dashed curve) plotted against the cochlear segments. The straight lines indicate the assumed linear regression of the diameter.

angle instead of length according to the so called “Cochlear View,” which was established for evaluation of the electrode insertion depth (19). According to this method, the round window lies on a reference line that passes through the center of the spiral at an angle of 10 degrees to the horizontal plane (20). Because full cochlear turns are defined via this reference line, every position in the cochlear spiral can be described in degrees (21). Consequently, the most anterior part of the cochlea equates to 170 degrees (Fig. 2).

Furthermore, the spiral of each individual cochlea was plotted in axial view. The width of the line represents the diameter of the greatest circle that could fit into the scala tympani. The diameter (width of the line) is scaled to the size of the spiral 1:2. These drawings were applied to compare measurement values and local micromorphology in selected segments of the cochlear duct. The reconstructed spirals are rotated by 90 degrees to correspond to the associated histologic sections (Fig. 5).

**Statistical Analysis**

The cochlear spiral was divided into segments, in each case representing 45 degrees. These parts were labeled according to the fraction of the corresponding full turns. For instance, the part from 0.01 to 45 degrees corresponds to 0.125, the part from 135.01 to 180 degrees corresponds to 0.500, and the part from 360.01 to 405 degrees corresponds to 1.125 (Fig. 2; Table 2).

For statistical analysis of the diameter of the scala tympani and the scala vestibuli, the mean for each segment in every cochlea was calculated. Means involving all cochleae were plotted in charts. To quantify the intersegmental change of the diameter, a linear regression over the whole spiral was assumed for every cochlea and compared with the effective intersegmental decrease by means of nonparametric statistics (Wilcoxon test). Under the null hypothesis, distributions of values do not differ between compared groups; otherwise, the null hypothesis was rejected with significance level at  $p \leq 0.05$  (2-tailed).

**RESULTS**

**Cross-Sectional Diameter**

Three thousand two hundred eighty-four measurement values were obtained. Although the absolute values for the diameter of each segment differed between the cochleae, the relative changes from segment to segment were similar through all series. In Figure 3, the mean cross-sectional diameter of the greatest circle that was fitted into the cochlear scalae is plotted against the cochlear segments. The diameter of the scala tympani decreases distinctly from segment 0.375 to segment 0.625, that is, within this quadrant, the diameter is reduced by approximately 300 µm (Table 1). From here, it remains constant until segment 1.375, where it increases locally by approximately 50 µm.

**TABLE 1.** Cross-sectional diameter (µm) of greatest circle fitted into the scala tympani and the scala vestibuli

Scala tympani					Scala vestibuli			
Mean	SD	Min	Max	Segment	Mean	SD	Min	Max
1,221.71	116.59	961.25	1,487.17	0.125	1,111.84	127.71	891.23	1,369.36
1,326.55	146.50	1,054.58	1,636.10	0.250	843.62	91.95	673.83	1,048.13
1,254.13	115.92	1,035.53	1,487.82	0.375	854.62	93.03	646.07	1,028.89
1,086.79	115.37	879.33	1,286.20	0.500	930.59	98.70	738.86	1,109.33
956.04	103.18	793.00	1,184.71	0.625	1,036.19	124.45	779.20	1,275.75
918.09	90.31	722.45	1,091.40	0.750	1,083.25	106.84	879.45	1,239.70
883.83	84.77	680.11	1,024.43	0.875	1,185.04	109.38	996.82	1,403.60
880.08	101.55	689.67	1,137.67	1.000	1,158.19	139.08	942.67	1,368.00
887.89	100.10	695.67	1,138.00	1.125	1,045.89	113.26	891.00	1,271.75
890.35	82.04	749.88	1,048.67	1.250	972.32	102.31	790.57	1,221.17
945.35	74.58	815.29	1,109.88	1.375	969.87	99.26	773.00	1,218.50
894.13	121.17	698.00	1,198.00	1.500	932.32	83.52	776.00	1,077.50
711.15	75.70	543.00	879.50	1.625	914.74	84.30	724.00	1,094.50
706.31	71.78	580.50	865.60	1.750	925.99	78.02	751.80	1,099.00
754.22	72.97	616.25	914.00	1.875	918.93	103.78	763.00	1,219.75
715.84	97.02	569.00	931.00	2.000	871.30	139.04	638.00	1,284.50
678.06	91.20	569.00	897.00	2.125	807.71	165.45	621.00	1,241.00
640.06	92.21	459.67	845.00	2.250	786.27	148.67	586.00	1,150.50
680.76	90.71	482.75	816.00	2.375	790.76	130.73	577.50	1,184.00
554.16	129.60	362.00	810.00	2.500	692.09	112.23	414.00	897.00

n = 3,284 measurements in 28 temporal bones.

Max indicates maximum diameter; Mean, mean of the diameter in the segment; Min, minimum diameter; SD, standard deviation.

The curve of the cross-sectional diameter of the scala vestibuli has an inverted course. The diameter drops within the first 2 segments and increases between segment 0.375 and segment 0.875. There, it reaches its maximum, followed by a steep decline until segment 1.250 and a less steep decline up to the end of the duct.

The assumed linear decrease of the cross-sectional diameter is 35.28  $\mu\text{m}$  per segment for the scala tympani and 22.17  $\mu\text{m}$  per segment for the scala vestibuli.

#### Variance From the Linear Decrease of Diameter

The regression of the cross-sectional diameter in the previously mentioned sections of the scala tympani was quantified. For every section, the diameter change to the previous one was calculated. The variance of these values in comparison with the assumed linear decrease of the scala tympani cross-sectional diameter is plotted in Figure 4. The decrease of the diameter exceeds linear regression by 132  $\mu\text{m}$  from segment 0.375 to segment 0.500 and by 95.5  $\mu\text{m}$  from segment 0.500 to segment 0.625. For both segments, the variance from a linear diameter regression is highly significant (Fig. 4).

#### Micromorphology

The area from segment 0.375 to segment 0.625 corresponds to the ascending part of the basal turn. The micromorphology of the affected segments was investigated in cochlear reconstructions in accordance with the corresponding histologic specimens (Fig. 5). The histologic sections can be localized in the spiral by means of the illustrated sectional planes (Fig. 5). Specimen "A" contains sections of the cochlear scalae from the previously mentioned segments 0.375 and 0.625. Specimen "B" shows segment 0.250, which features the maximum cross-sectional diameter of the scala tympani in the basal turn, and segment 0.875, which marks the end point of the preceding regression of scala tympani diameter.

Although cross-sectional diameter and shape of the bony capsule of the cochlear duct remain nearly constant through the evaluated segments, the diameters of the scala tympani and the scala vestibuli change inversely. Regard-

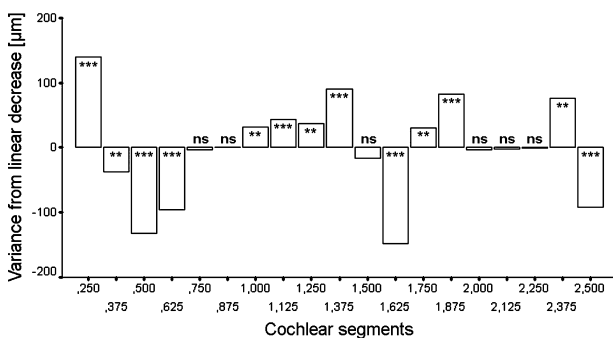


**FIG. 4.** Cross-sectional diameter of scala tympani segments. Variance between the diameter-change referred to the previous segment in comparison to the assumed linear decrease of cross-sectional diameter. Level of significance:  $p > 0.05$  (NS);  $*p \leq 0.05$ ;  $**p \leq 0.01$ ,  $***p \leq 0.001$ .

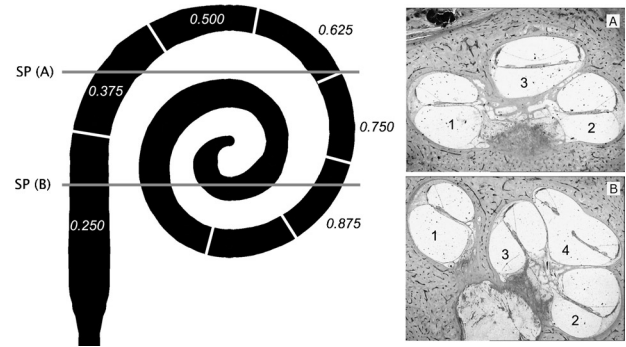


**FIG. 5.** Path of the greatest diameter of circles that can be matched into a left human scala tympani (left) with sketched sectional planes (SP) of selected histologic specimens (right; A, B): The half-turns of the scala tympani are numbered 1 to 4, and the cochlear sections are labeled as described in the text. The scale of the spiral to the scale of the diameter is 2:1.

ing half-turns 1 and 2, the osseous spiral lamina shifts toward the scala tympani. Whereas the size of the cross-sectional shape of the scala tympani decreases, the shape of the scala vestibuli enlarges and forms a small peak due to the close relationship between the first and the second cochlear turn. However, when the diameters of both scalae are summarized and the results are plotted against the cochlear segments in a diagram (not shown), a shallow dip in the plotted curve between segment 0.125 and segment 0.875 results.

The appearance of the reconstructed cochleae is inhomogeneous (not shown) with variable coiling patterns and different lengths of the hook region. In some series, local variations of the cross-sectional diameter of the scala tympani, which differed from the previously described pattern, could be observed. Figure 6 shows the reconstruction of the scala tympani from a right ear with a localized narrowing in the hook region. On several histologic sections, an osteoma-like protrusion, which is located opposite to the spiral osseous lamina and covers a distance of 1,120  $\mu\text{m}$ , protrudes from the bony capsule of the scala tympani. The largest circle that can be superimposed in this particular area has a diameter of 1,054  $\mu\text{m}$ , whereas the mean cross-sectional diameter for this segment (0.125) is 1,221.71  $\mu\text{m}$ .

## DISCUSSION

### Methodological Considerations

In 2-dimensional specimens, the width of the cochlear scalae (parallel to the spiral lamina) can only be assessed correctly in a midmodiolar section (Fig. 1). In all adjacent sections, the lumen is cut obliquely, and, therefore, measurements of the width reveal higher values than is correct; the height of the lumen (perpendicular to the spiral lamina) remains unaffected. However, because the height of the scalae is less than the width throughout the length of the cochlea (22), the diameter of an electrode with circular cross section is limited by the height.



**FIG. 6.** Reconstruction of a right human scala tympani (top) and associated histologic section (bottom): On the image of the histologic specimen, *asterisk* marks a bony protrusion. The resulting local narrowing is indicated on the spiral by the *arrow*. The half-turns of the cochlear duct are numbered 1 to 3.

The graphic reconstruction method of the cochlea has frequently been used in temporal bone research for more than 80 years. It allows localization inside the cochlea in reference to the cochlear spiral on the base of histologic sections. Minor errors in measuring the length of the cochlear duct were described by Guild (17) and Schuknecht (18). Takagi and Sando (23) emphasized that an oblique cutting angle of the cochlea causes additional errors for length measurement. If a temporal bone is not sectioned parallel to the plane of the modiolus, the apparent diameters of the turns measured on the graphic reconstruc-

tion are smaller than the actual ones, and therefore, calculation of the length reveals reduced values. To avoid these inaccuracies, positioning inside the cochlea was referred to the angle instead to a metric distance for the paper presented here. However, even if the length of a part of the cochlear duct, in particular the hook region, can only be estimated with less accuracy due to methodological issues, this has no relevance for higher segments because the angle is referenced to the beginning of every half-turn of the cochlea.

In most electrode insertion studies, the insertion depth angle or a similar reference system with fractionized cochlear turns is used. Since the “Cochlear View” was established for postoperative radiography, this method of referencing positions inside the cochlea is ready for use in clinical application (19). To improve the clinical usability, results from anatomic investigations of the cochlear micromorphology should be expressed with regard to the (insertion depth) angle.

**Dimensions of the Cochlear Scalae**

It is widely known that the diameter of the cochlear duct decreases from the base of the cochlea to the apex. However, the decrease does not proceed linearly. In fact, several expansions and narrowings can be observed, differing from an assumed linear regression of the cross-sectional diameters (Fig. 3). Reports on the cochlear dimensions from other authors vary slightly due to different reference systems and definitions of distances inside the cochlea. Walby (16) gives an overview regarding several studies and presents a chart with the data from other authors. It is evident that, although the maxima and minima of the curves appear at different positions, the curves would fairly coincide if a standardized reference system were used. To allow comparison between the present findings and previous studies, the angular reference system was related to distance measurements inside the cochlear duct (Table 2).

The inverse measurements of both perilymphatic scalae are a constant finding during the first 1½ turns. According to Wysocki (22), this observation is even more distinct if one considers the cross-sectional area of the scalae. The progression of the diameters was discussed in detail by several authors. Walby (16) reports on decreasing height of the scala tympani up to 9 mm distance from the round window. Because he measured the distance in the middle of the scala, this area corresponds to segment 0.500 of the cochlear spiral. Wysocki (22) observed this regression up to 12- to 13-mm distance from the beginning of the

**TABLE 2.** Comparison of different reference systems for localization in the cochlear spiral

Angle, degrees	90	180	270	360	450	540	630	720	810	900
End of segment	0.250	0.500	0.750	1.000	1.250	1.500	1.750	2.000	2.250	2.500
ST inner wall, mm	6.03	9.05	11.67	13.53	15.05	16.14	16.99	17.67	17.96	18.17
ST outer wall, mm	7.92	13.85	19.25	23.32	27.07	30.21	33.18	35.81	38.37	40.25

Data for length of ST inner and outer wall are obtained from Kawano et al. (34). ST indicates scala tympani.

scala. According to Zrunek and Lischka (24) and Zrunek et al. (25), the height of the scala tympani decreases from 1.4 mm at approximately 6 to 7 mm from the round window to 0.84 mm at 17 to 18 mm. Wysocki and Zrunek measured the distance on the outer wall of the perilymph cast. Therefore, these measurements correspond to segments 0.500 and 0.625. The narrowing that was observed by Hatsushika et al. (26) was limited to the first 1.5 to 2 mm.

However, many researchers focused mainly on the so-called "bottleneck" of the scala tympani between the initial narrowing and an expansion occurring in the region at 70 to 80% from the base of the cochlea (16). The rapid narrowing of the scala tympani in the region of the ascending part of the basal turn was not regarded as the remarkable feature of the cochlear duct. We could demonstrate that the reduction of the cross-sectional diameter from segment 0.375 to segment 0.500 and from segment 0.500 to segment 0.625 significantly exceeds the linear regression of the diameter (Fig. 4), a finding that has not been reported previously.

Obviously, the steep decrease of the cross-sectional diameter of the scala tympani between segment 0.375 and segment 0.625 is induced by a combination of narrowing of the bony capsule and shifting or rotation of the spiral osseous lamina (27). A slight reexpansion of the bony capsule, beginning from segment 0.750, compensates the influence of the lamina spiralis ossea on the diameter of the scala tympani. These findings are conclusive with Erixon et al. (14). They evaluated corrosion casts of human cochleae and reported on impressions occurring in the pars ascendens of the basal turn. The authors attributed these findings to imprints of the carotid canal, which approximates the otic capsule in the area of the ascending part of the basal turn from 0 to 4.1 mm (mean, 1.08 mm) (28). Examination of the spatial relationship between otic capsule and carotid canal was not feasible in our specimens due to the vertical sectioning plane.

From the literature, case reports on bony dehiscences between the cochlear basal turn and the carotid canal are known, and radiologic assessment of the so-called "cochlear-carotid interval" revealed corresponding measurements from 0 to 5 mm (29,30). The distance between cochlea and carotid canal varies, although the rapid narrowing of the scala tympani was a constant finding in our measurements. However, the role of the periotic mesenchyme in otic morphogenesis is still not adequately understood (31). The proximity of the carotid artery may influence the cavitation of the cochlear duct during embryology. Additionally, Muren et al. (32) reported on impressions in the wall of the carotid canal opposite to the cochlea, which may be another advice for interactions between otic capsule and carotid canal during development.

#### Correlation to Typical Patterns of Insertional Trauma

Although the development of electrode insertion trauma is influenced by different factors, for example, electrode design or insertion technique, the occurrence of severe injuries at a location approximately 180 degrees from the

round window is regarded a typical pattern (6,8,9). Even with improved electrode designs, at least minimal injuries appear, in particular, in the region of the ascending part of the basal turn (10). The advantage of precurved electrode arrays, which were held straight by a stylet before insertion, may be explained by the potential not only to lead the array smoothly around the first bend of the cochlear duct but also to guide it through the accompanying narrowing (11,33). Furthermore, the mechanical features of the electrode array play a role, for example, improved flexibility, which may reduce friction in higher turns and therefore lead to less buckling of the array, mainly in the region of segment 0.500 and segment 0.650 of the cochlear duct (7). The localized narrowing of the scala tympani in this area may contribute to this effect.

#### CONCLUSION

The absolute values of cross-sectional diameter vary between individuals. This obviously contributes to the failure of preformed electrode arrays. For optimization of electrode design and insertion technique, the knowledge regarding variations in diameter from a linear progression of the cochlear duct, which are constant between individuals, is important. We observed a significant increase of the linear regression of scala tympani diameter in the region of the ascending part of the basal turn. From the literature, it is known that electrode insertion trauma frequently occurs here. The task of guiding the electrode array around the first bend of the cochlear turn is challenged by the local narrowing. Therefore, our finding should be considered for the development of electrode design and insertion methods. Additionally, if further studies confirmed a positive correlation between diameter of scala tympani and cochlea-carotid interval, it would be feasible to derive information regarding critical intracochlear dimensions from standard radiologic investigations.

**Acknowledgments:** The author thanks U. Koch, M.D., Ph.D., M. Sanchez-Hanke, M.D., Ph.D., A. Münscher, M.D. (Department of ORL, University Medical Centre Hamburg-Eppendorf, Hamburg, Germany), and H.-P. Schmiedebach, M.D., Ph.D. and A. Zare, M.A. (Department of History and Ethics of Medicine, University Medical Centre Hamburg-Eppendorf, Hamburg, Germany) for providing the histologic specimens.

#### REFERENCES

1. Cullen RD, Higgins C, Buss E, Clark M, Pillsbury HC, Buchman CA. Cochlear implantation in patients with substantial residual hearing. *Laryngoscope* 2004;114:2218–23.
2. Balkany TJ, Connell SS, Hodges AV, et al. Conservation of residual acoustic hearing after cochlear implantation. *Otol Neurotol* 2006;27:1083–8.
3. Leake PA, Rebscher SJ. Anatomical considerations of electrical stimulation. In: Zeng FG, Popper AN, Fay RR, eds. *Cochlear Implants—Auditory Prosthesis and Electric Hearing*. New York, NY: Springer, 2004:101–48.
4. Eshraghi AA. Prevention of cochlear implant electrode damage. *Curr Opin Otolaryngol Head Neck Surg* 2006;14:323–8.
5. Roland PS, Wright CG. Surgical aspects of cochlear implantation:

- mechanisms of insertional trauma. In: Moller AR, ed. *Cochlear and Brainstem Implants*. Basel, Switzerland: Karger, 2006:11–30.
6. Eshraghi AA, Yang NW, Balkany TJ. Comparative study of cochlear damage with three perimodiolar electrode designs. *Laryngoscope* 2003;113:415–9.
  7. Roland JT. A model for cochlear implant electrode insertion and force evaluation: results with a new electrode design and insertion technique. *Laryngoscope* 2005;115:1325–39.
  8. Stover T, Issing P, Graurock G, et al. Evaluation of the advance off-stylet insertion technique and the cochlear insertion tool in temporal bones. *Otol Neurotol* 2005;26:1161–70.
  9. Wardrop P, Whinney D, Rebscher SJ, Roland JT, Luxford W, Leake PA. A temporal bone study of insertion trauma and intracochlear position of cochlear implant electrodes. I: Comparison of Nucleus banded and Nucleus Contour electrodes. *Hear Res* 2005;203:54–67.
  10. Wardrop P, Whinney D, Rebscher SJ, Luxford W, Leake P. A temporal bone study of insertion trauma and intracochlear position of cochlear implant electrodes. II: Comparison of Spiral Clarion and HiFocus II electrodes. *Hear Res* 2005;203:68–79.
  11. Wright CG, Roland PS, Kuzma J. Advanced bionics thin lateral and Helix II electrodes: a temporal bone study. *Laryngoscope* 2005;115:2041–5.
  12. Adunka OF, Pillsbury HC, Kiefer J. Combining perimodiolar electrode placement and atraumatic insertion properties in cochlear implantation—fact or fantasy? *Acta Otolaryngol* 2006;126:475–82.
  13. Biedron S. Evaluation of the cochlear micro morphology and the internal dimensions of the cochlear scalae with special reference to insertional trauma during cochlear implantation [in German]. *Thesis, RWTH Aachen University*. Aachen, Germany, 2008:202.
  14. Erixon E, Hogstorp H, Wadin K, Rask-Andersen H. Variational anatomy of the human cochlea: implications for cochlear implantation. *Otol Neurotol* 2009;30:14–22.
  15. Eckart-Möbius A. Gehörorgan. In: Henke F, Lubarch O, eds. *Die pathologisch-anatomische Untersuchungstechnik und die normal-histologischen Grundlagen. Handbuch der speziellen pathologischen Anatomie und Histologie*. Berlin, Germany: Springer, 1926.
  16. Walby AP. Scala tympani measurement. *Ann Otol Rhinol Laryngol* 1985;94:393–7.
  17. Guild S. A graphic reconstruction method for the study of the organ of Corti. *Anat Rec* 1921;22:141–57.
  18. Schuknecht HF. Techniques for study of cochlear function and pathology in experimental animals; development of the anatomical frequency scale for the cat. *AMA Arch Otolaryngol* 1953;58:377–97.
  19. Xu J, Xu SA, Cohen LT, Clark GM. Cochlear view: postoperative radiography for cochlear implantation. *Am J Otol* 2000;21:49–56.
  20. Cohen LT, Xu J, Xu SA, Clark GM. Improved and simplified methods for specifying positions of the electrode bands of a cochlear implant array. *Am J Otol* 1996;17:859–65.
  21. Adunka O, Unkelbach MH, Mack MG, Radeloff A, Gstoettner W. Predicting basal cochlear length for electric-acoustic stimulation. *Arch Otolaryngol Head Neck Surg* 2005;131:488–92.
  22. Wysocki J. Dimensions of the human vestibular and tympanic scalae. *Hear Res* 1999;135:39–46.
  23. Takagi A, Sando I. Computer-aided three-dimensional reconstruction: a method of measuring temporal bone structures including the length of the cochlea. *Ann Otol Rhinol Laryngol* 1989;98:515–22.
  24. Zrunek M, Lischka M. Dimensions of the scala vestibuli and sectional areas of both scales. *Arch Otolaryngol* 1981;233:99–104.
  25. Zrunek M, Lischka M, Hochmair-Desoyer I, Burian K. Dimensions of the scala tympani in relation to the diameters of multichannel electrodes. *Arch Otolaryngol* 1980;229:159–65.
  26. Hatsushika S, Shepherd RK, Tong YC, Clark GM, Funasaka S. Dimensions of the scala tympani in the human and cat with reference to cochlear implants. *Ann Otol Rhinol Laryngol* 1990;99:871–6.
  27. Shepherd RK, Franz BK, Clark GM. The biocompatibility and safety of cochlear prostheses. In: Clark GM, Tong YC, Patrick JF, eds. *Cochlear Prostheses*. London, UK: Churchill Livingstone, 1990:69–98.
  28. Fichtl H. Lagebeziehungen, Variationen und Masse der Kanalsysteme in der Pars petrosa des Os temporale. *Thesis, Julius-Maximilians-University*. Würzburg, Germany, 1991.
  29. Modugno GC, Brandolini C, Cappello I, Pirodda A. Bilateral dehiscence of the bony cochlear basal turn. *Arch Otolaryngol Head Neck Surg* 2004;130:1427–9.
  30. Young RJ, Shatzkes DR, Babb JS, Lalwani AK. The cochlear-carotid interval: anatomic variation and potential clinical implications. *AJNR Am J Neuroradiol* 2006;27:1486–90.
  31. Mansour SL, Schoenwolf GC. Morphogenesis of the inner ear. In: Kelley MW, Wu DK, Popper AN, Fay RR, eds. *Development of the Inner Ear*. New York, NY: Springer, 2002.
  32. Muren C, Wadin K, Wilbrand HF. The cochlea and the carotid canal. *Acta Radiol* 1990;31:33–5.
  33. Roland JT, Fishman AJ, Alexiades G, Cohen NL. Electrode to modiolus proximity: a fluoroscopic and histologic analysis. *Am J Otol* 2000;21:218–25.
  34. Kawano A, Seldon HL, Clark GM. Computer-aided three-dimensional reconstruction in human cochlear maps: measurement of the lengths of organ of Corti, outer wall, inner wall, and Rosenthal's canal. *Ann Otol Rhinol Laryngol* 1996;105:701–9.